

COMP9517: Computer Vision

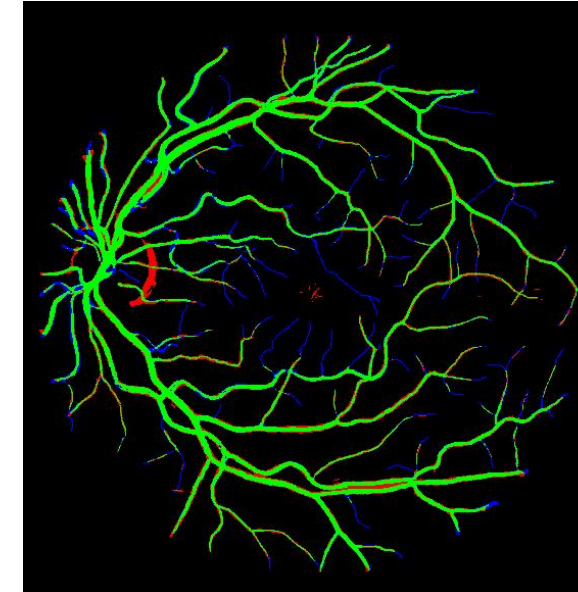
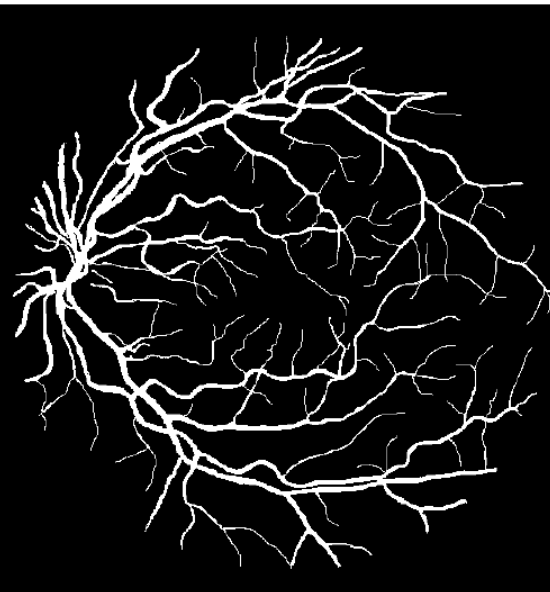
Applications of Computer Vision
Week 9 (Part 1)

Tariq M. Khan



UNSW
SYDNEY

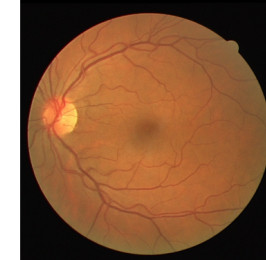
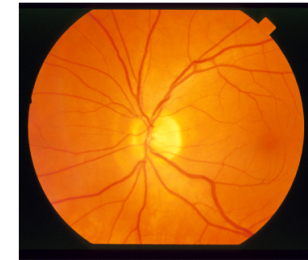
Image Segmentation Objective



- True positives
- True negatives
- False positives
- False negatives

Medical Image Segmentation Challenges

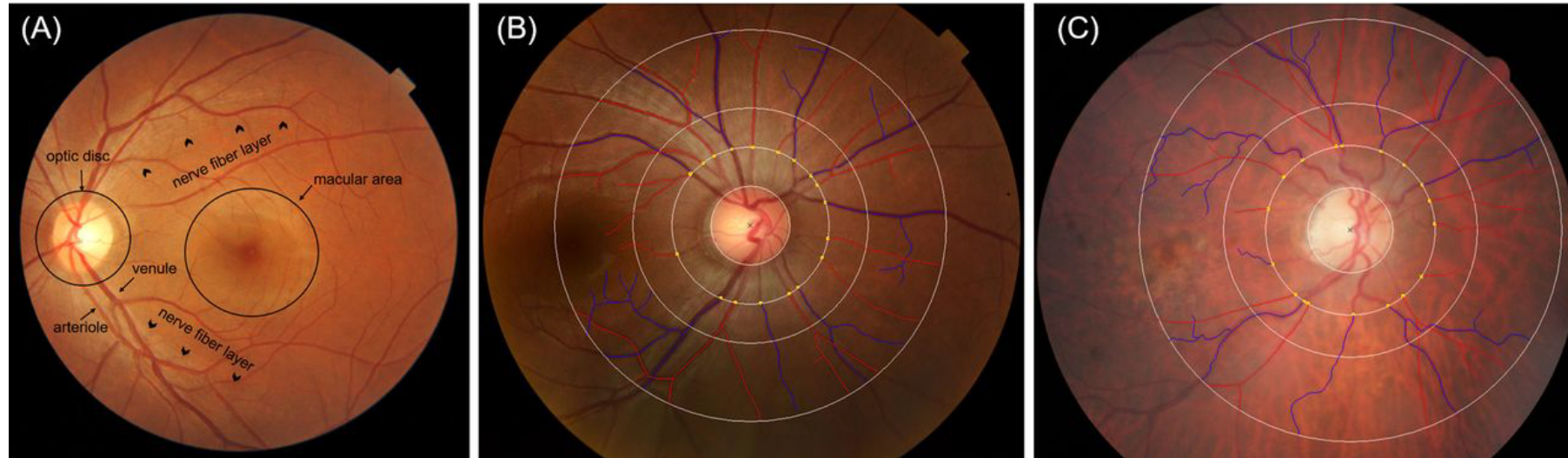
- Structural boundary ambiguity
- Heterogeneous texture
- Segmented area uncertainties
- Intensity inhomogeneity
- Large contrast variations
- Large image size



Medical Image Segmentation challenges

- Training and testing can be computationally expensive
- Down-sampling before training is usually required which is particularly undesirable in medical imaging

Retinal imaging in Alzheimer's disease

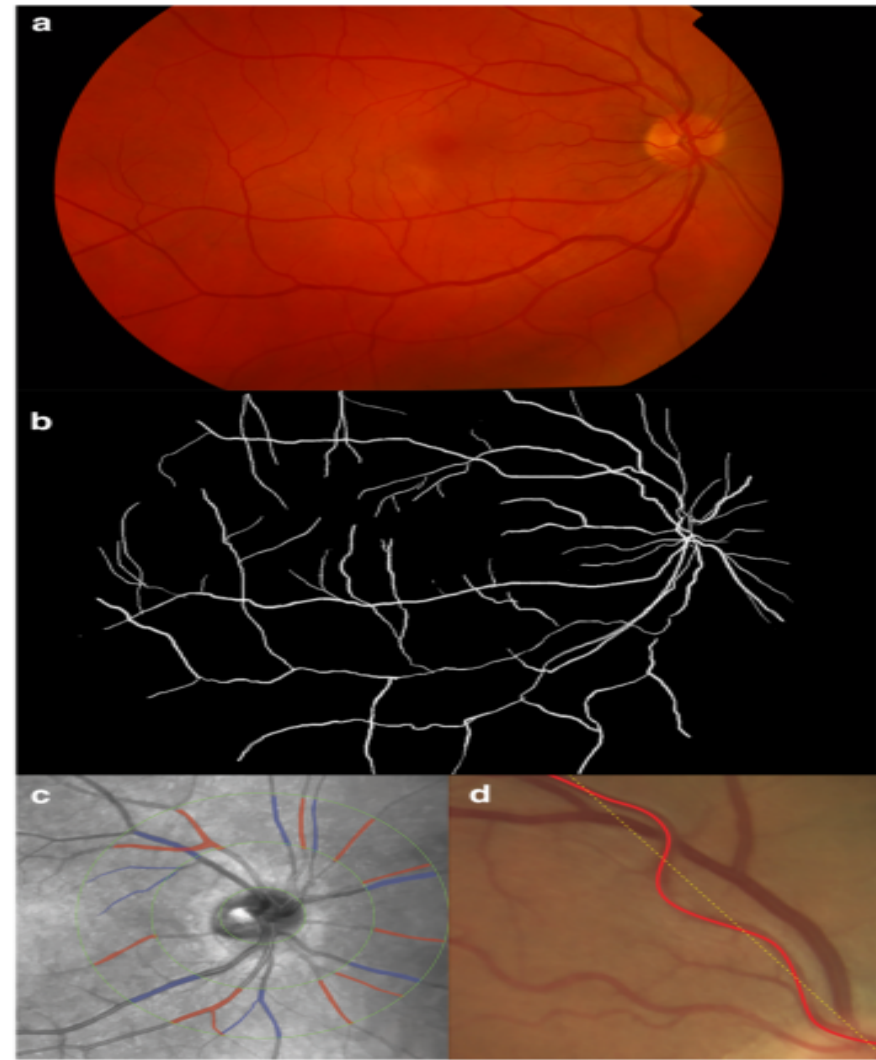


(A) Retinal photograph showing the optic nerve head, macular area, nerve fibre layer, arterioles and venules.

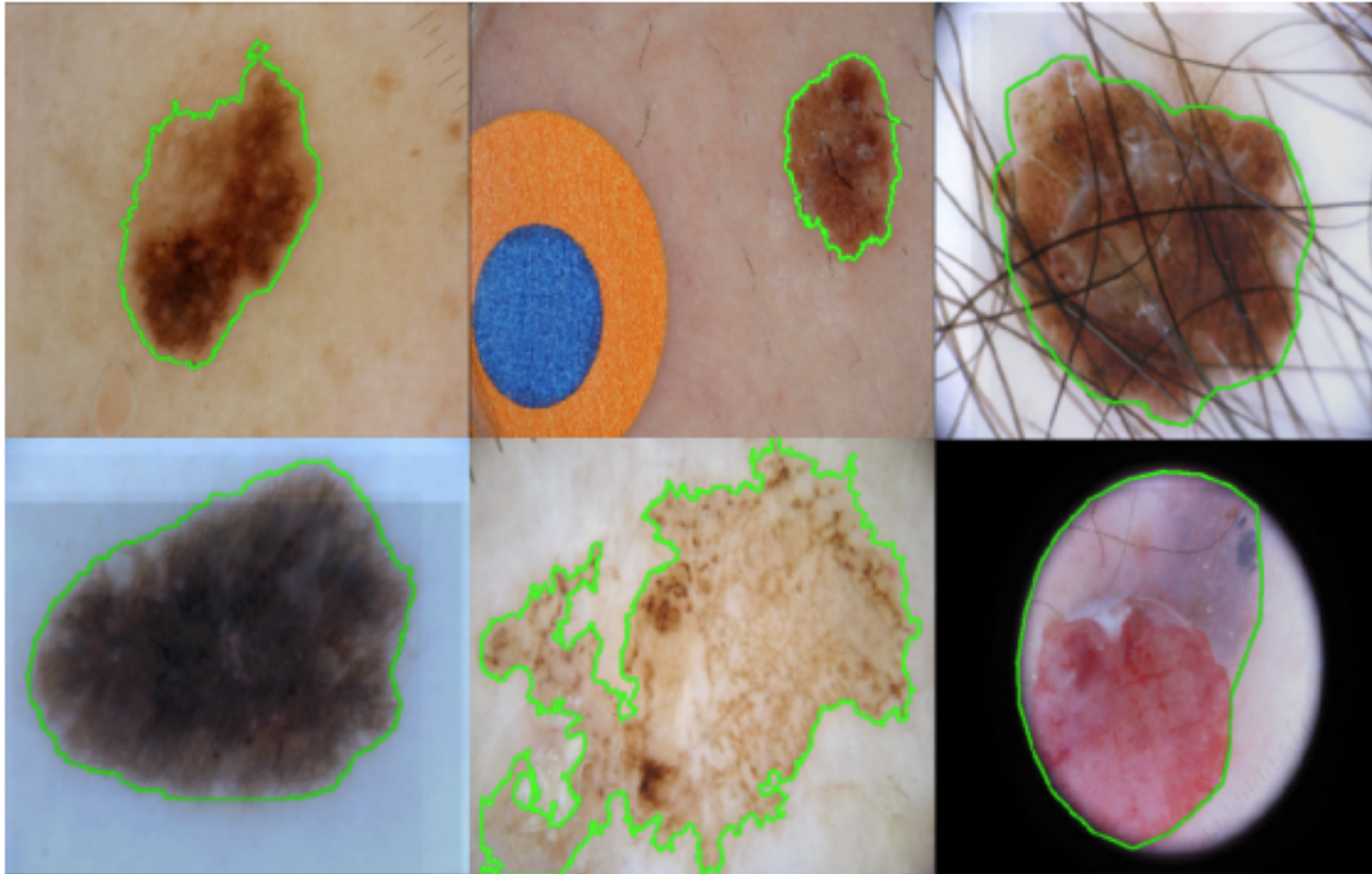
Carol Y Cheung et al. J Neurol Neurosurg Psychiatry
2021;92:983-994

Retinal imaging in Alzheimer's disease

Retinal vessel analysis: fundus photography (a) and skeletonized image of retinal vascular network for fractal analysis (b). The retinal fractal dimension (FD) is a measure of vasculature branching pattern complexity. Identification and measurement of retinal arteriole and venule caliber (c). The red and blue shadings indicate the selected arteriole and venule area, respectively. Measurement of retinal vascular tortuosity (d) that is derived from the integral of the curvature square along the vessel tracings, normalized by the total path length measured in a specified area.



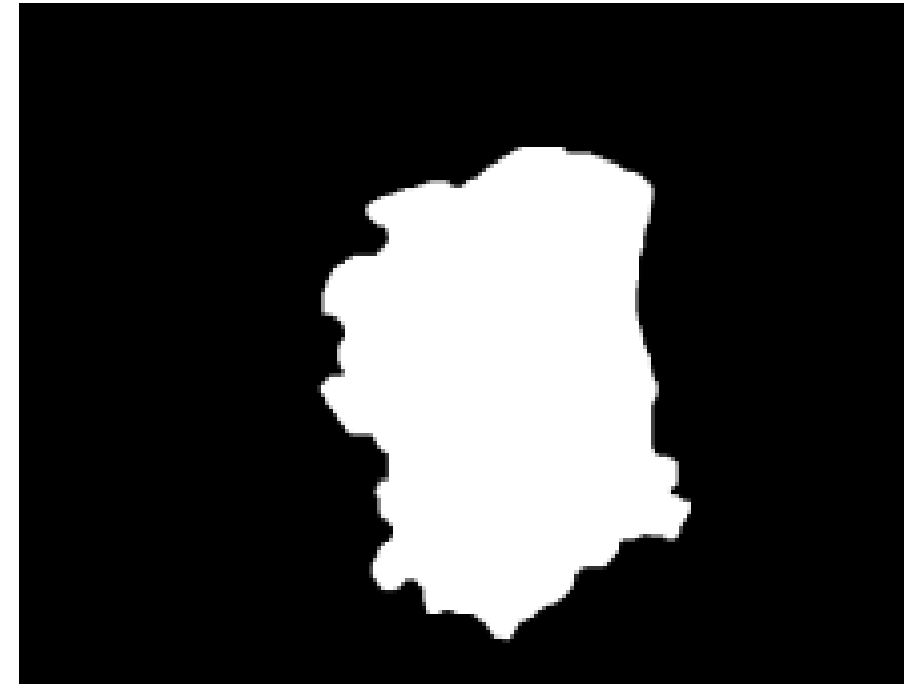
Skin Lesion Segmentation



Skin Lesion Segmentation

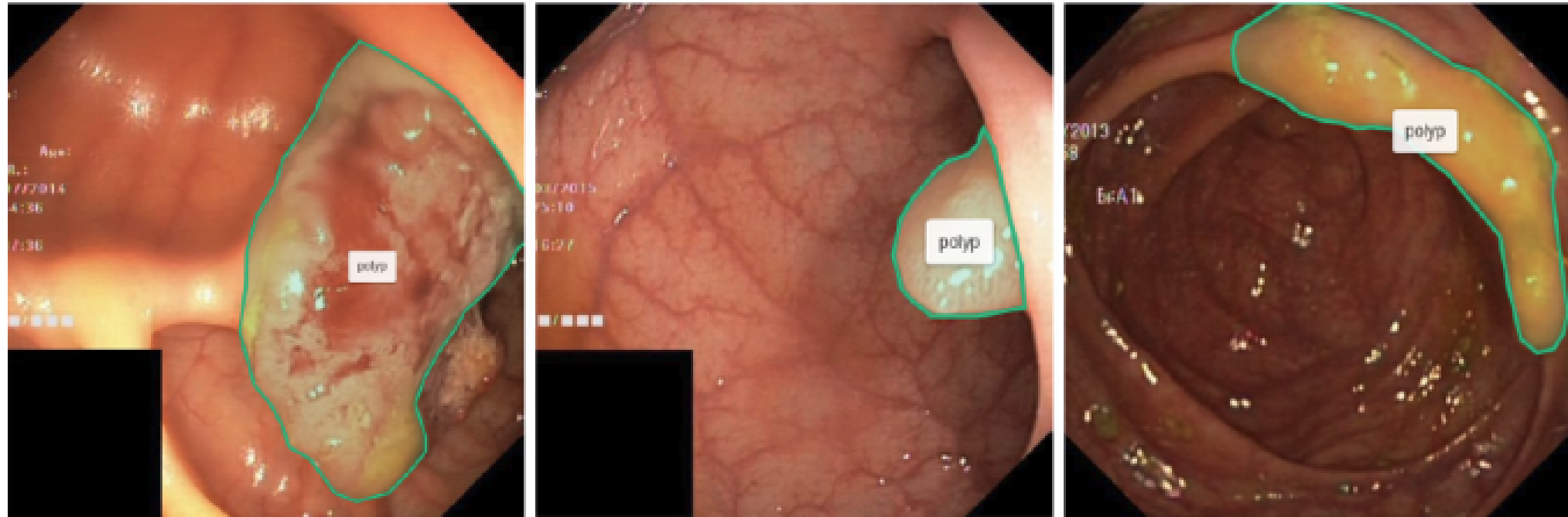


(a) Raw dermoscopy image

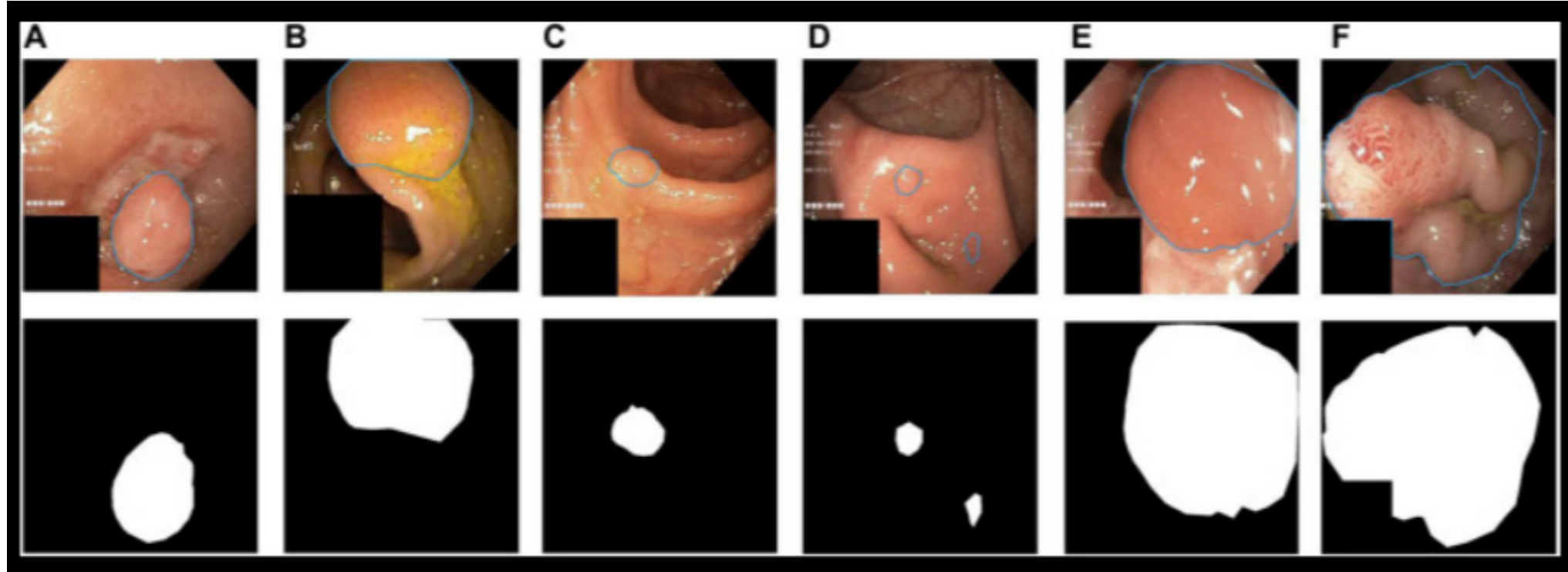


(b) Ground truth mask

Segmentation of Polyps in Gastrointestinal Tract Images

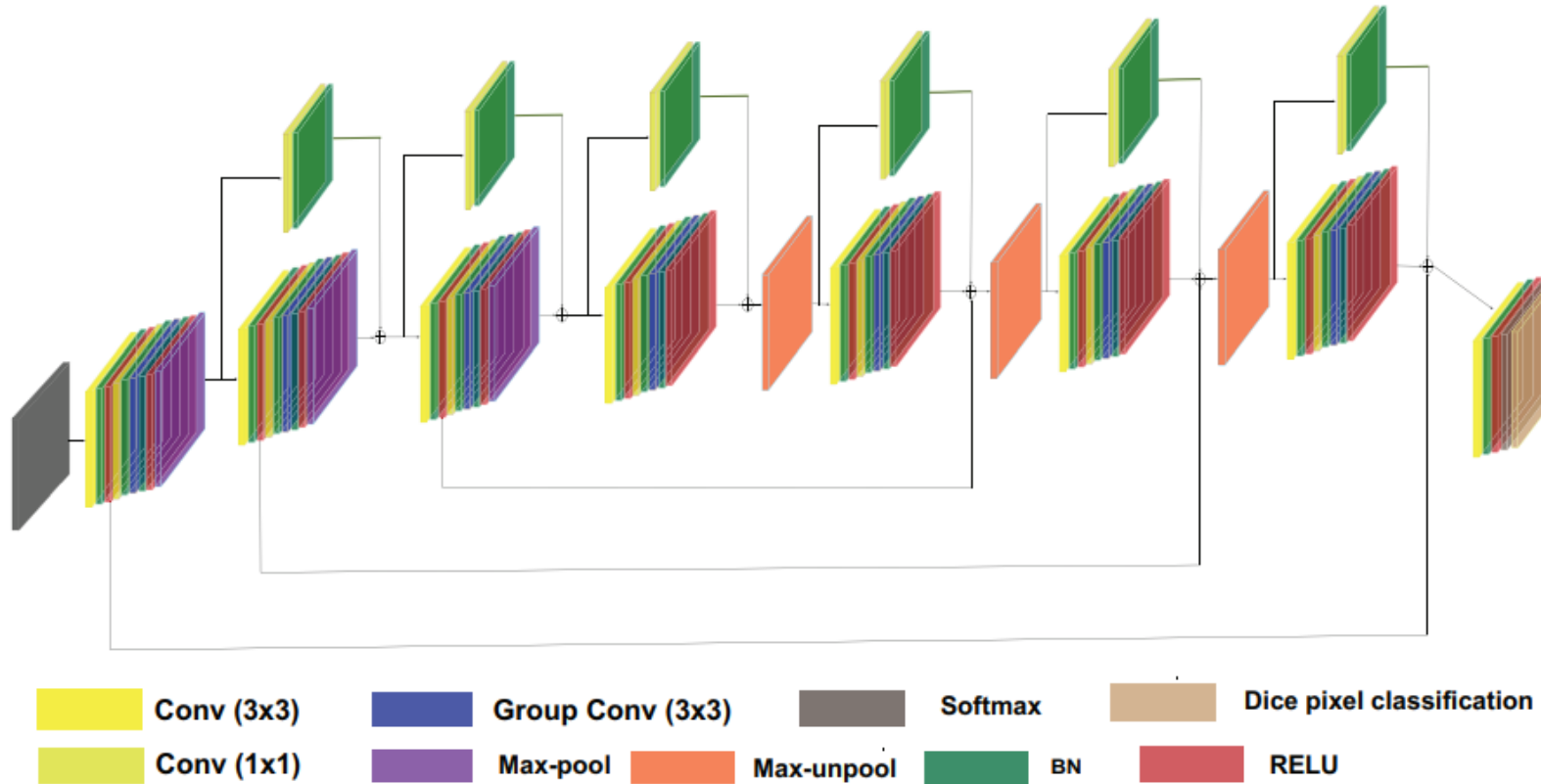


Segmentation of Polyps in Gastrointestinal Tract Images



Typical challenging examples of polyp segmentation results: **(A,B)** the polyps with low contrast to the background, **(C,D)** the small polyps, and **(E,F)** the large polyps.

T-Net



Preserving Boundary Information

- Boundary information at the convolutional block level is preserved through residual skip connections comprised of a 1×1 convolutions and a batch normalization operation.
- Grouped convolutional layers are used for channel-wise separable (also known as depth-wise separable) convolution.

Dice Coefficient Loss

- We use the loss given by:

$$\mathcal{L} = \sum_{I \in \mathcal{I}} (1 - D_I)^2 \quad (1)$$

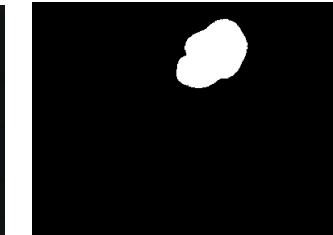
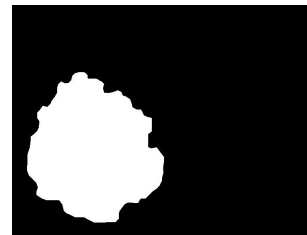
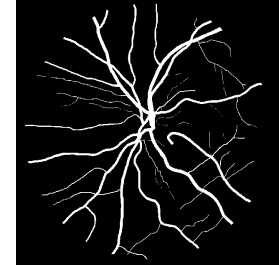
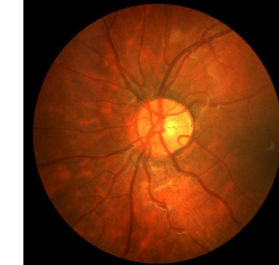
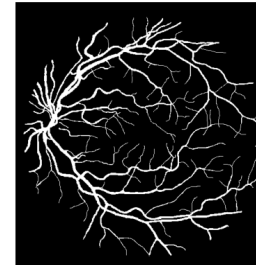
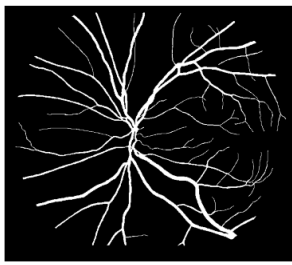
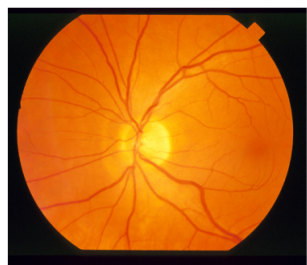
where D_I is the Dice coefficient for the image I in the dataset \mathcal{I} under consideration.

Recall the Dice coefficient is a scalar ranging from 0 to 1 which can be written as:

$$D_I = \frac{2 \sum_{i \in I} y_i \hat{y}_i}{\sum_{i \in I} y_i^2 + \sum_{i \in I} \hat{y}_i^2}$$

where y_j represents the predicted binary segmentation label for the i^{th} pixel in the image $I \in \mathcal{I}$ and \hat{y}_i denotes the corresponding ground truth.

Datasets



Filters effect

Filters	Se	Sp	Acc	F1-score	Layers	Parameters
T-Net {64, 128, 256}	0.8258	0.9834	0.9695	0.8257	81	2228870
T-Net {32, 64, 128}	0.8284	0.9828	0.9693	0.8250	81	596482
T-Net {16, 32, 64}	0.8281	0.9825	0.9689	0.8233	81	150278
T-Net {8, 16, 32}	0.8251	0.9816	0.9678	0.8180	81	35270
T-Net {8, 16, 24}	0.8262	0.9862	0.9697	0.8269	81	25910
T-Net {8, 16, 24} without skip connections	0.8270	0.9822	0.9689	0.8232	66	23886

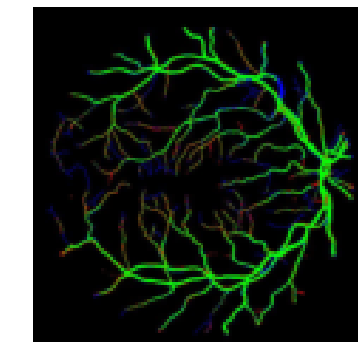
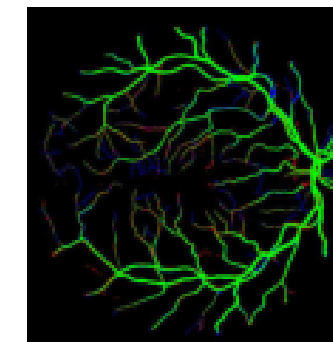
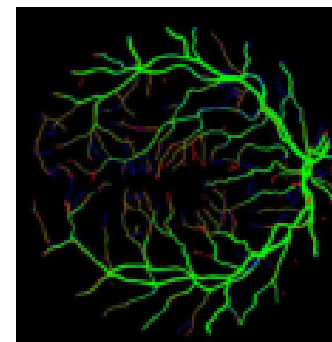
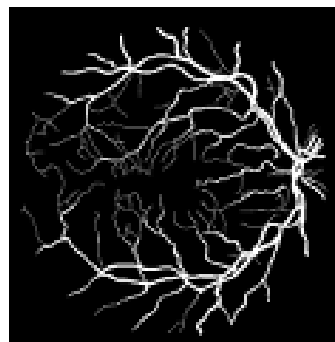
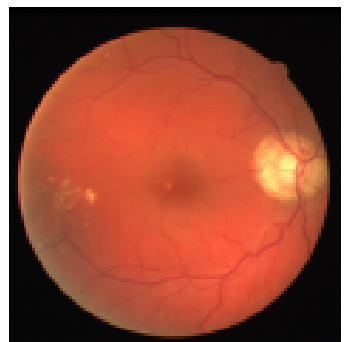
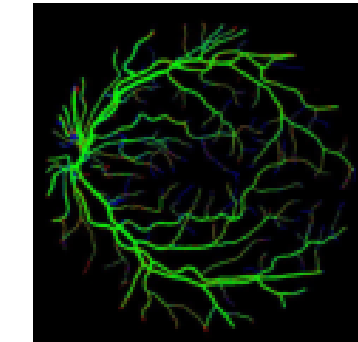
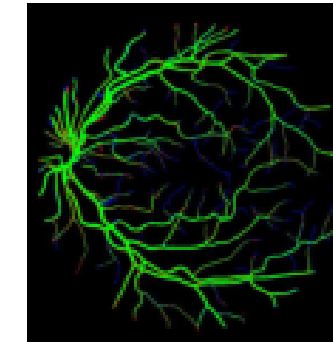
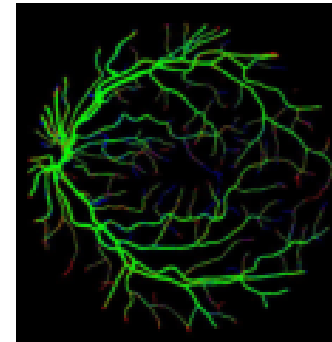
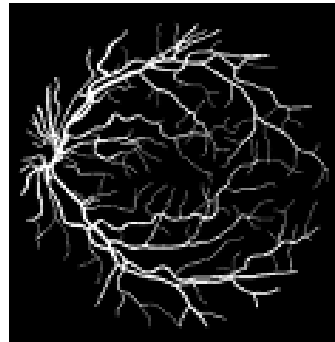
Table 1: Results yielded by T-Net for different filter configurations when applied to the DRIVE dataset

Initial Learning Rate

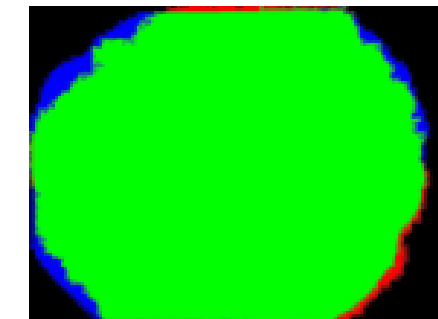
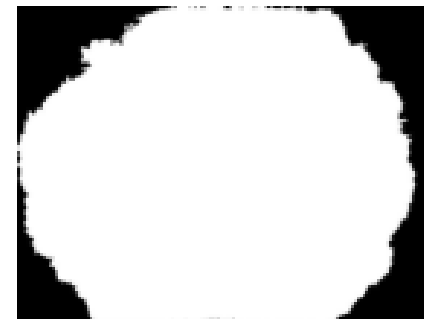
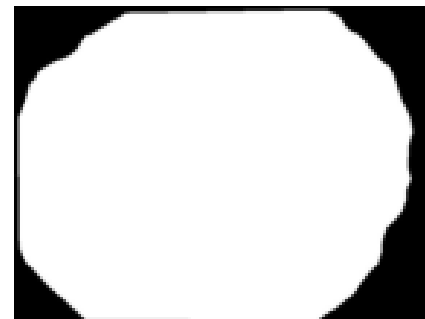
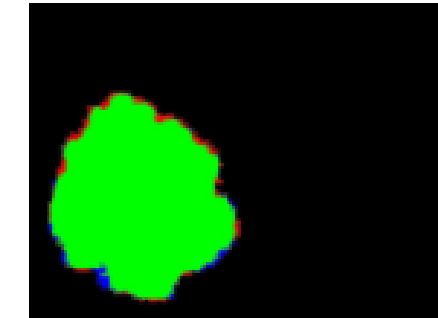
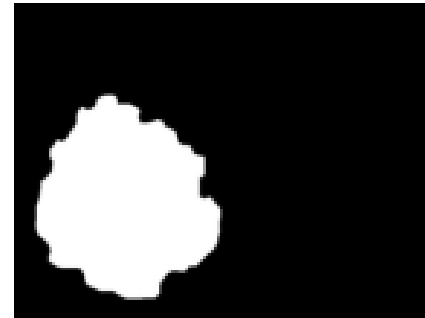
ILR	Se	Sp	Acc	F1 score
$1e^{-04}$	0.8247	0.9824	0.9685	0.8208
$2e^{-04}$	0.8286	0.9821	0.9687	0.8224
$3e^{-04}$	0.8263	0.9828	0.9690	0.8235
$4e^{-04}$	0.8307	0.9825	0.9691	0.8250
$5e^{-04}$	0.8283	0.9828	0.9693	0.8251
$6e^{-04}$	0.8254	0.9826	0.9689	0.8225
$7e^{-04}$	0.8277	0.9825	0.9689	0.8233
$8e^{-04}$	0.8313	0.9821	0.9688	0.8237
$1e^{-03}$	0.8262	0.9862	0.9697	0.8269
$2e^{-03}$	0.8281	0.9826	0.9690	0.8238

Table 2: Results for different initial learning rates (ILR) on the DRIVE dataset

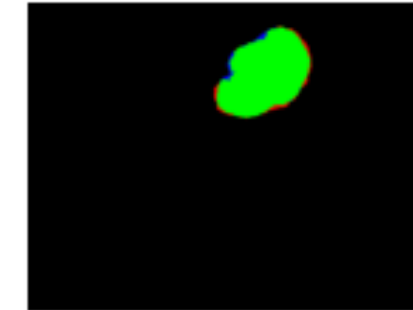
Visual Results (Retinal Vessel Segmentation)



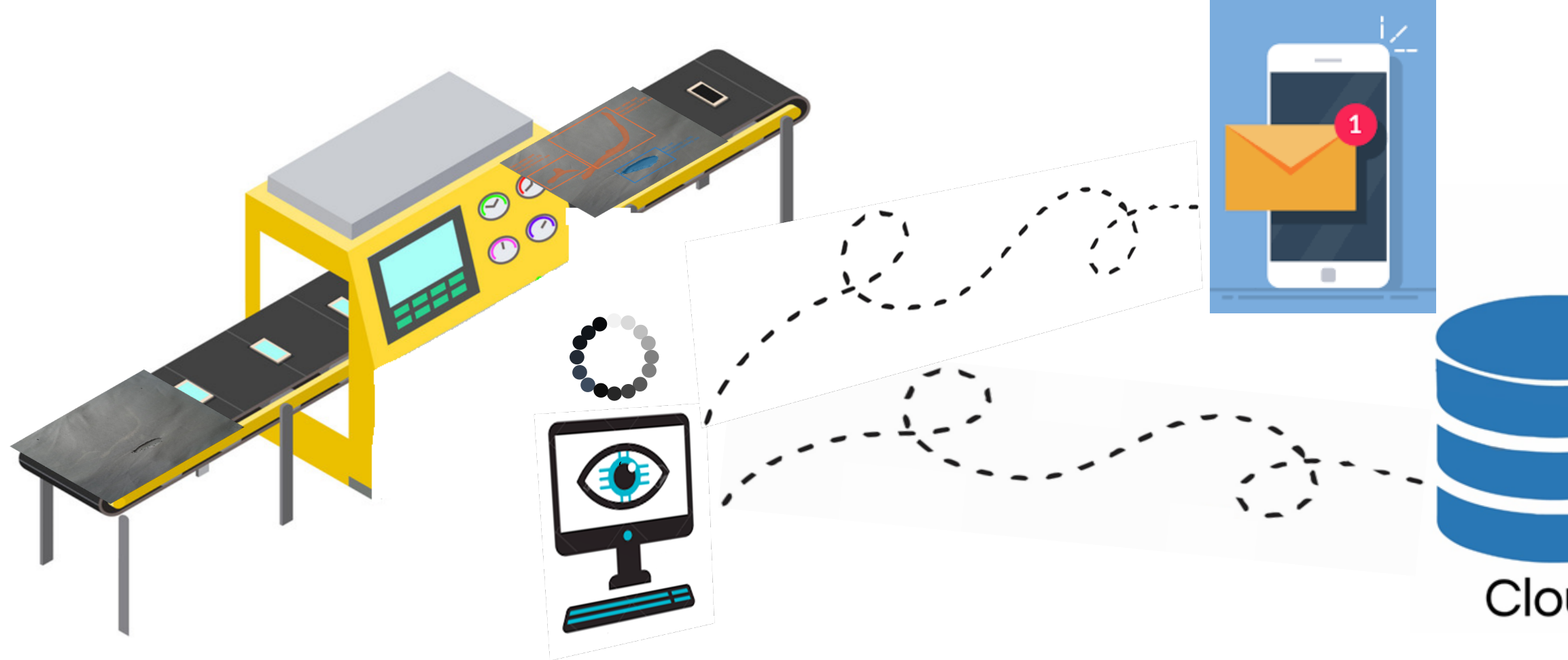
Visual Results (Skin Lesion Segmentation)



Visual Results (Digestive Tract Polyp Segmentation)

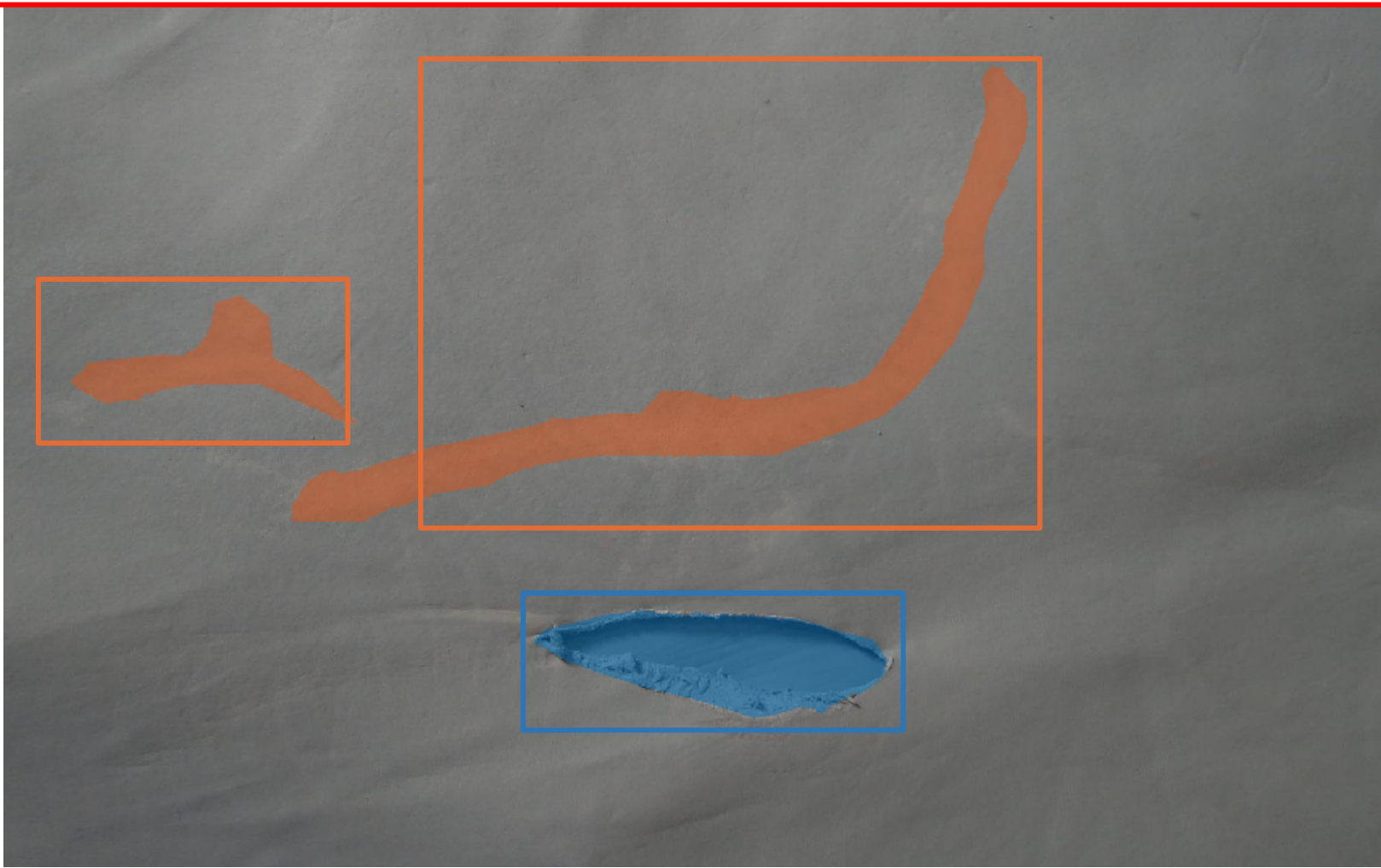


Leather Hide Grading System





ud



Grading Report

Type: white spots

Covered Area: more than 20%

Distance from corner: xx

Type: cuts

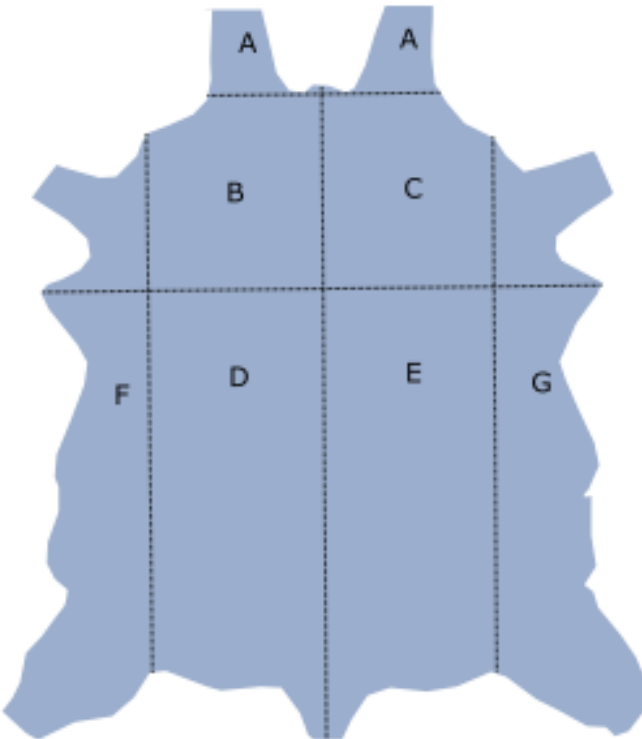
Covered Area: less than 10%

Distance from corner: xx

Overall grade: 4

Confidence: xx%

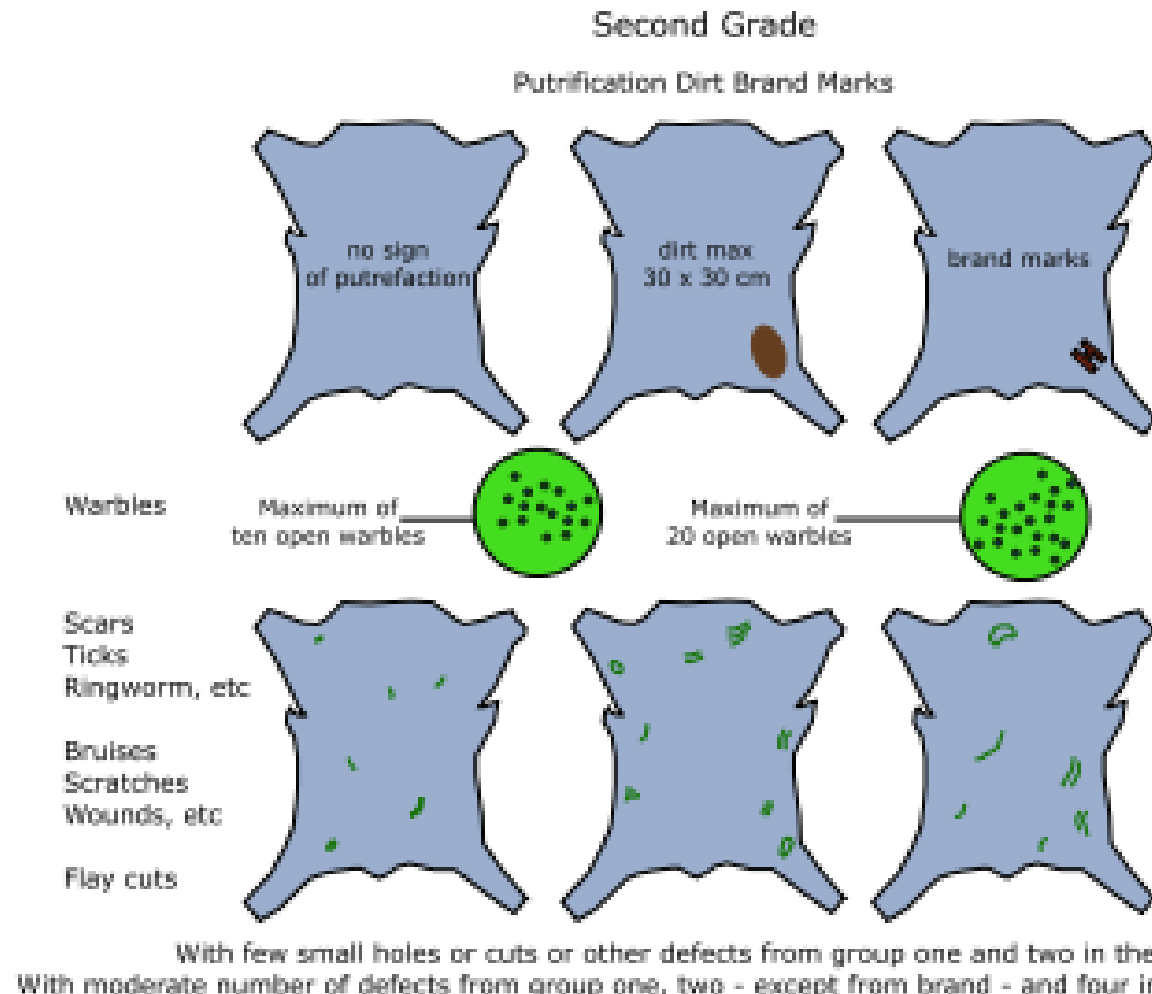
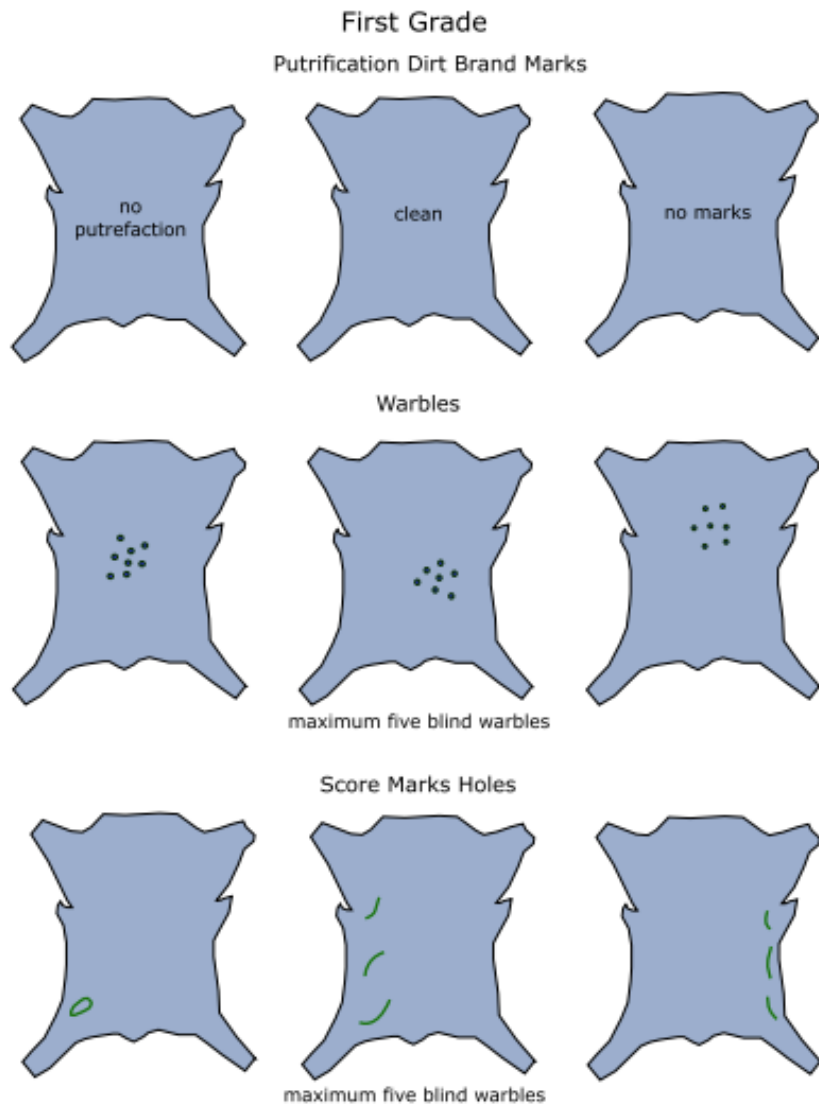
Subdivisions of a hide



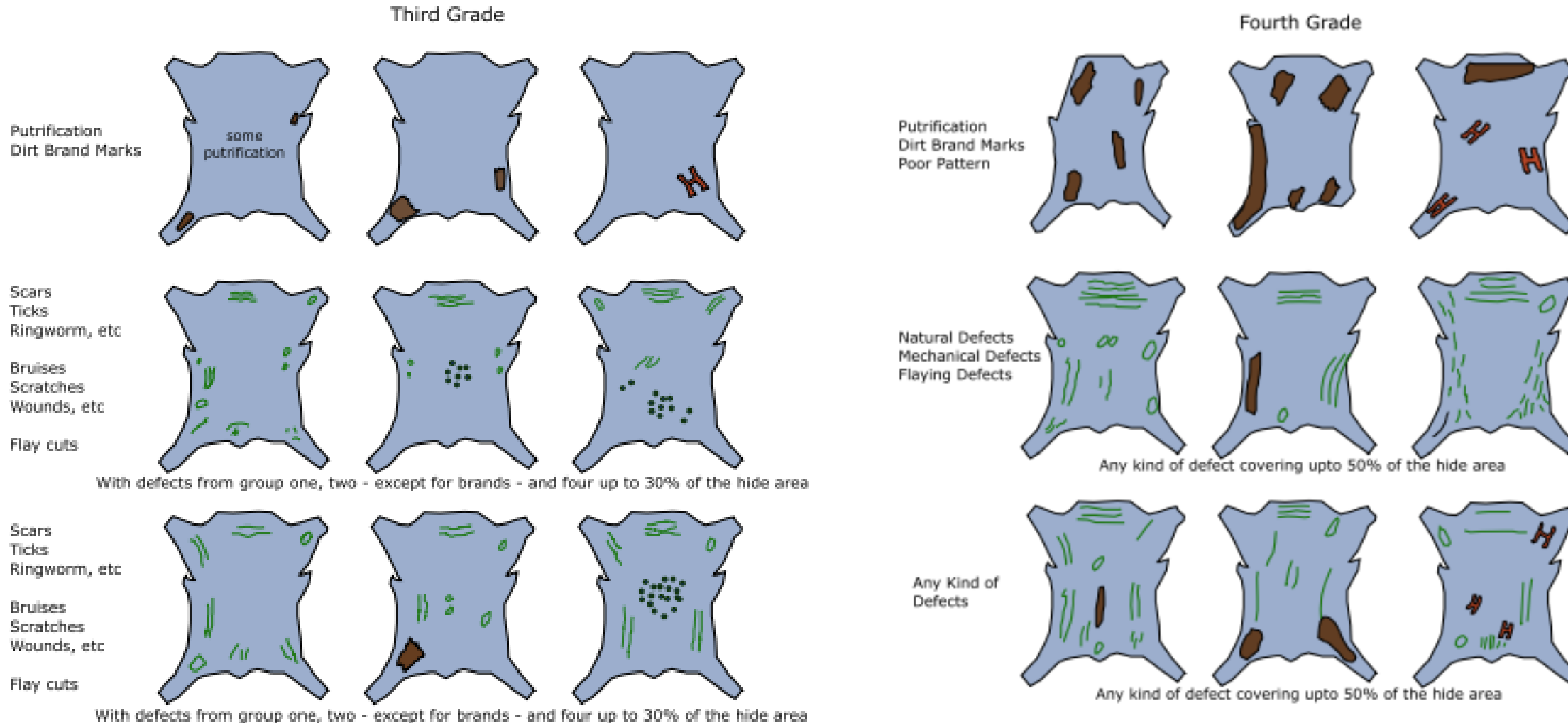
Head A
Shoulder B+C
Bend D or E
Belly F or G
Side A+B+D+F or A+C+G

Crop A+B+D or A+C+E
Back B+D or C+E
Croupon D+E
Dosset B+C+D+E+A
Culatta D+E+F+G

Grading Criteria



Grading Criteria



Examples of defects in wet blue leather



(a)



(b)



(c)



(d)



(e)



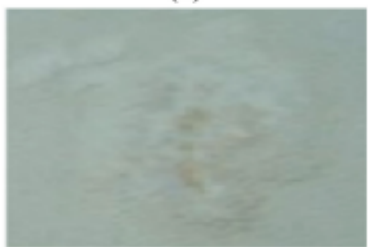
(f)



(g)



(h)



(i)



(j)



(k)



(l)



(m)



(n)



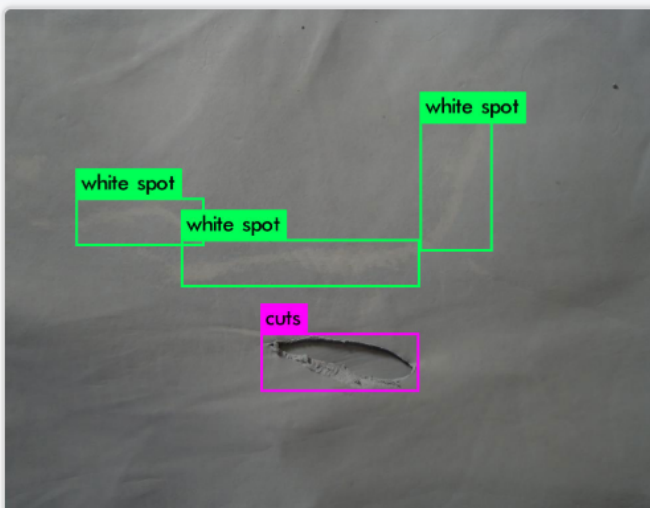
(o)



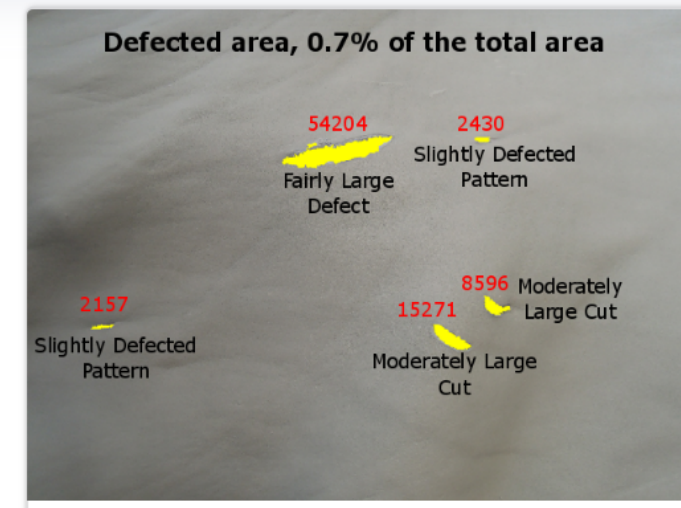
(p)



Leather Sample Categorization



Leather Defect Localization



Leather defect analysis

Overall pipeline for leather visual defect inspection - a guideline for machine vision systems

